Electronic Supplementary Information

In-situ transformation of Fe-doped $Ni_{12}P_5$ into low-crystallized $NiFe_2O_4$with high-spin $Fe^{4+}$for efficientlyelectrocatalyticwater oxidation

Haojie Wang,[a] Cuijiao Zhao,[a] Guozhong Wang,[a] and Haimin Zhang[a†]

[a] *Key Laboratory of Materials Physics, Centre for Environmental and Energy Nanomaterials, Anhui Key Laboratory of Nanomaterials and Nanotechnology, CAS Center for Excellence in Nanoscience, Institute of Solid State Physics, HFIPS, Chinese Academy of Sciences, Hefei 230031, China.*

[†]Corresponding author. E-mail: zhanghm@issp.ac.cn

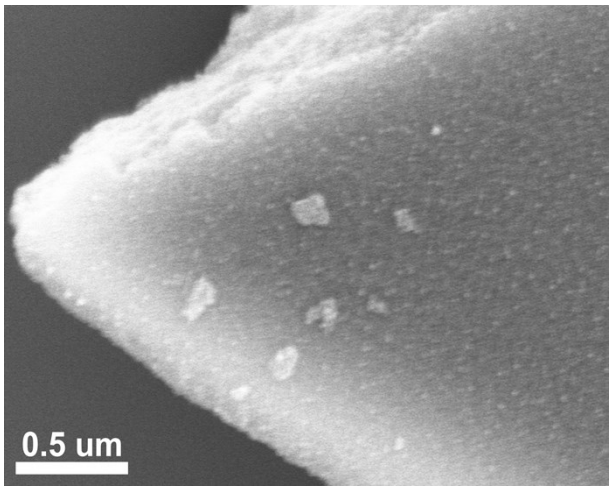

Fig. S1 SEM image of as-fabricated $(Fe_{0.25}Ni_{0.75})_{12}P_5$@PPC.

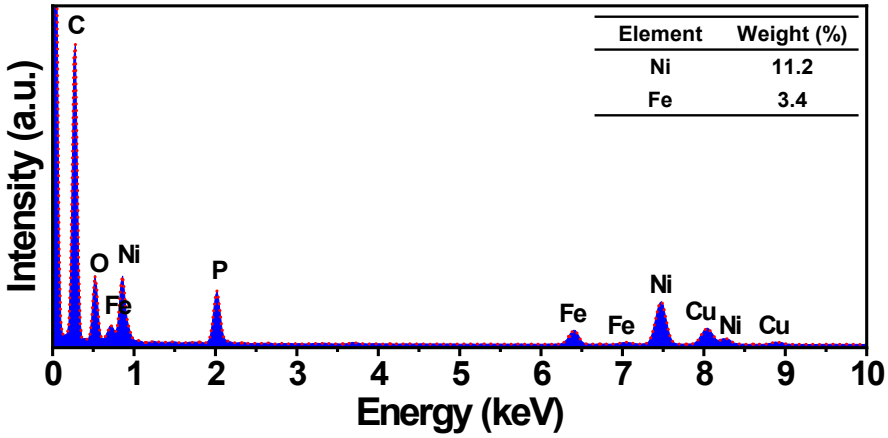

Fig. S2 EDX spectrum of as-fabricated $(Fe_{0.25}Ni_{0.75})_{12}P_5$@PPC.

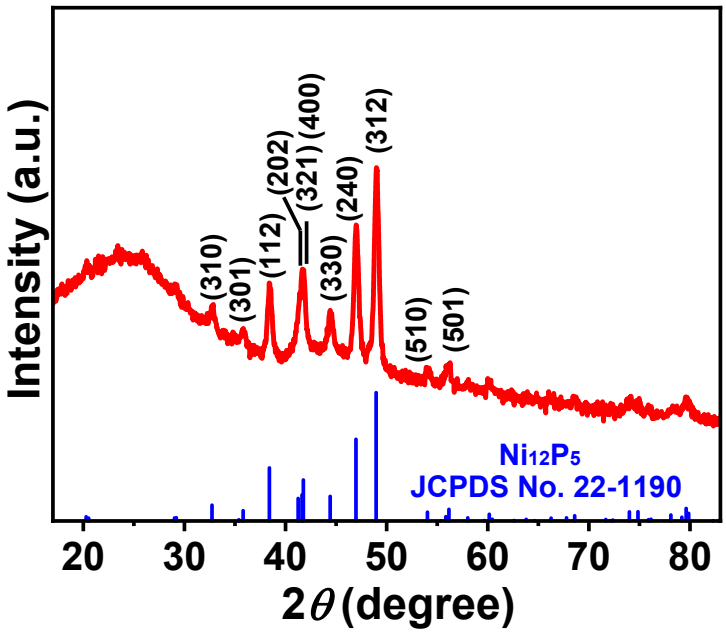

Fig. S3 XRD patterns of as-fabricated $(Fe_{0.25}Ni_{0.75})_{12}P_5$@PPC.

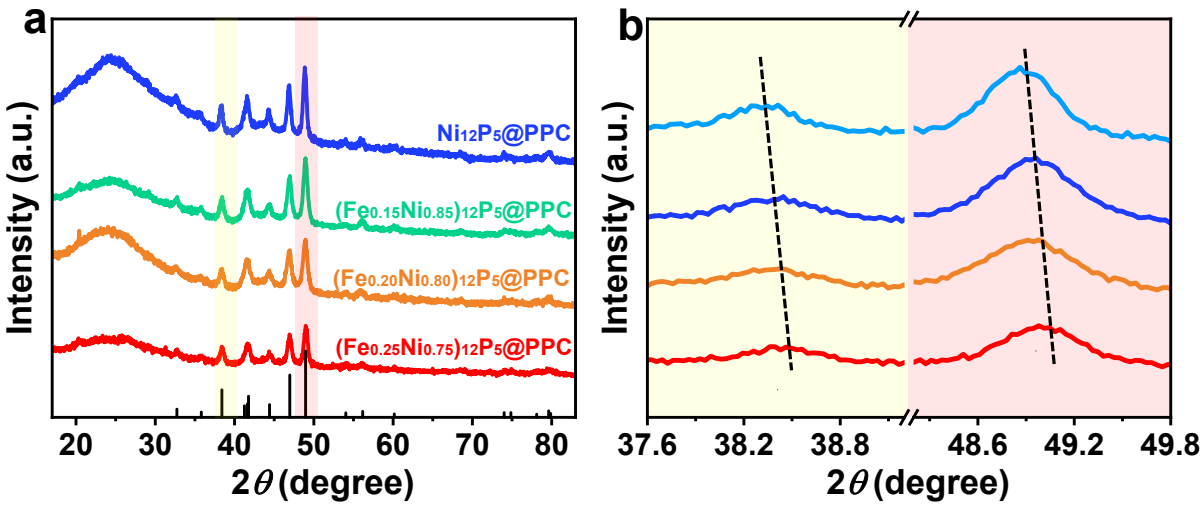

Fig. S4 (a) XRD patterns of $(Fe_xNi_y)_{12}P_5$@PPC (x= 0, 0.15, 0.20, 0.25; y=1, 0.85, 0.80, 0.75) and (b) Corresponding partial enlarged XRD patterns.

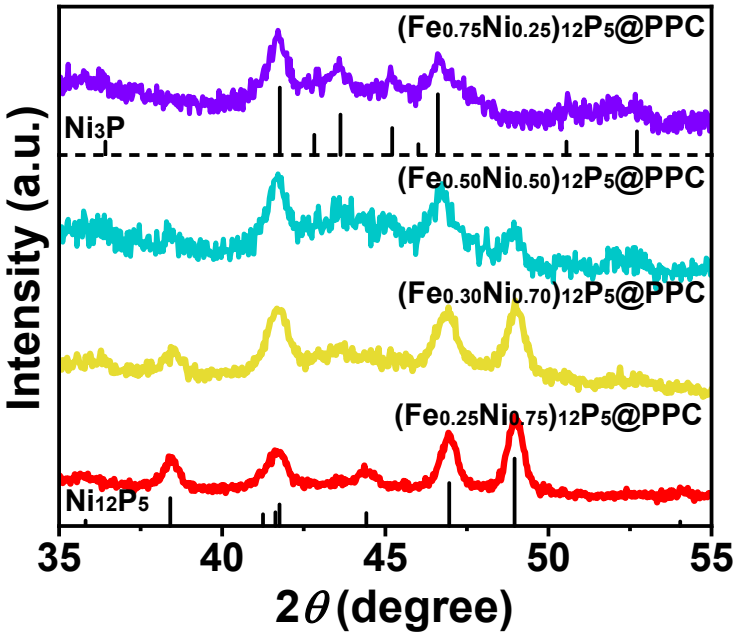

Fig. S5 XRD patterns of the fabricated samples with Fe amount over 0.25 in $(Fe_xNi_y)_{12}P_5$@PPC.

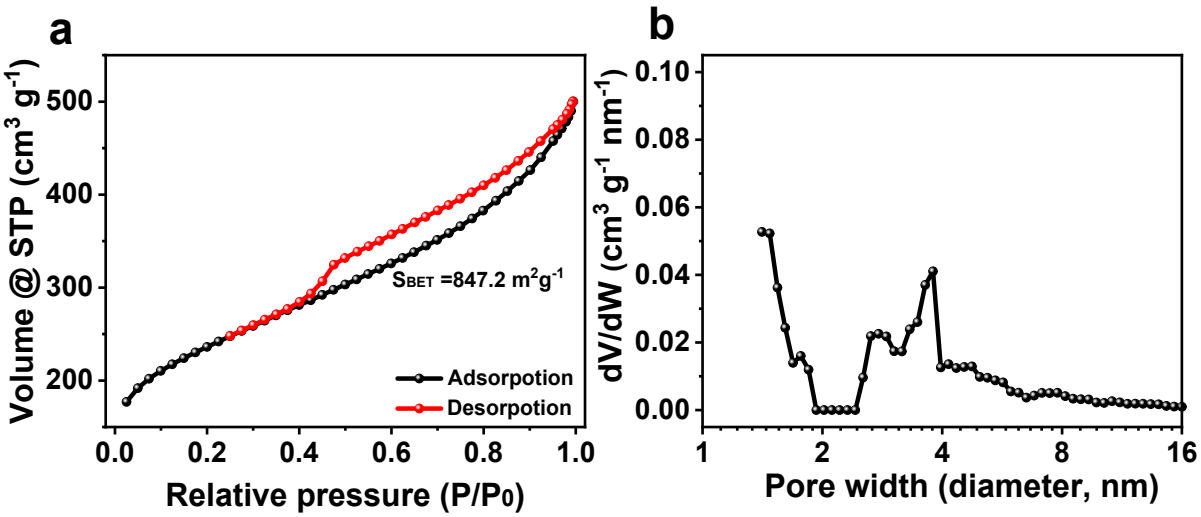

Fig. S6 (a) N_2 adsorption-desorption isotherm and (b) Corresponding DFT pore size distribution curve of $(Fe_{0.25}Ni_{0.75})_{12}P_5$@PPC.

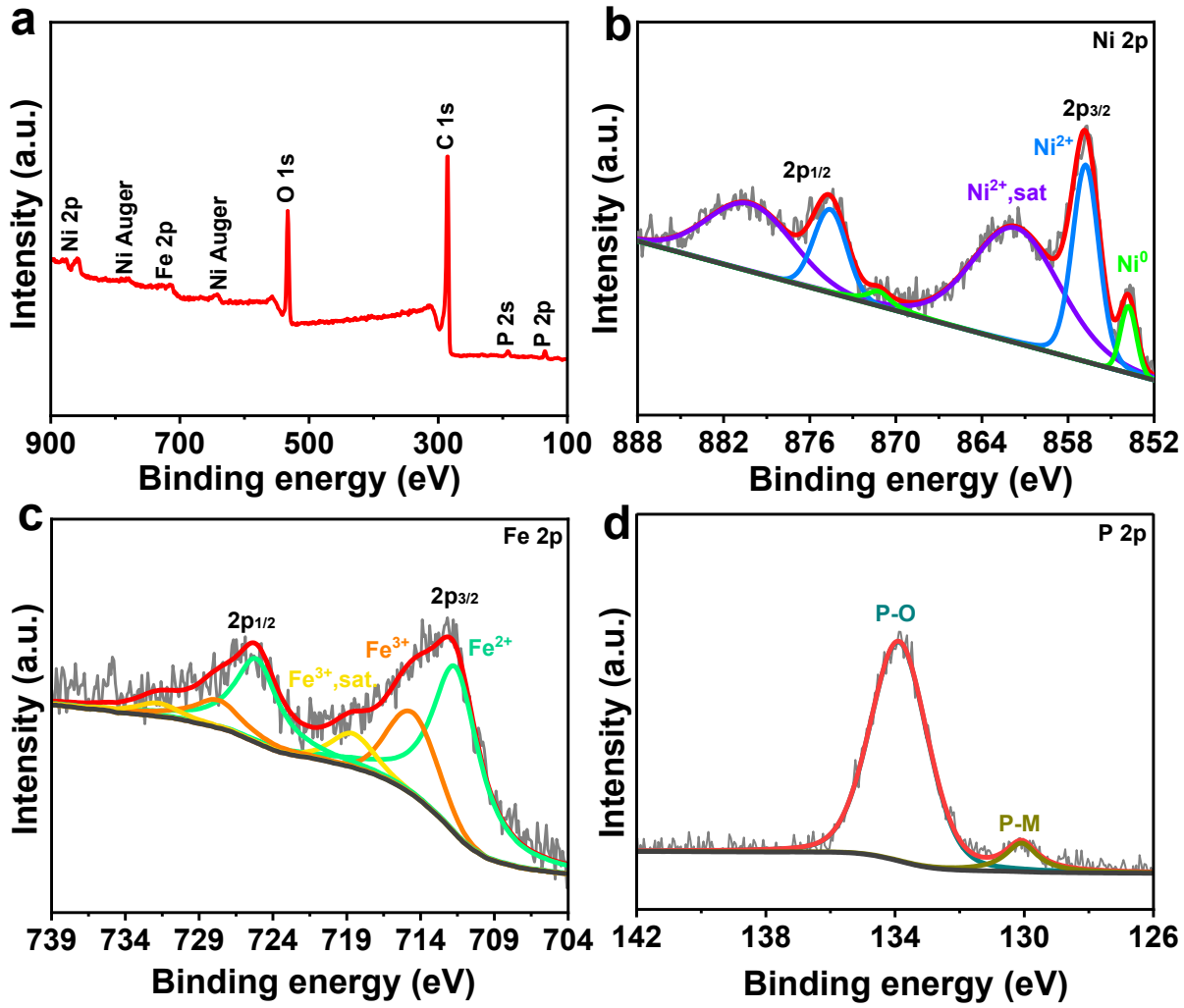

Fig. S7 (a) XPS survey spectrum and corresponding high-resolution (b) Ni 2p, (c) Fe 2p, and (d) P 2p XPS spectra of $(Fe_{0.25}Ni_{0.75})_{12}P_5$@PPC.

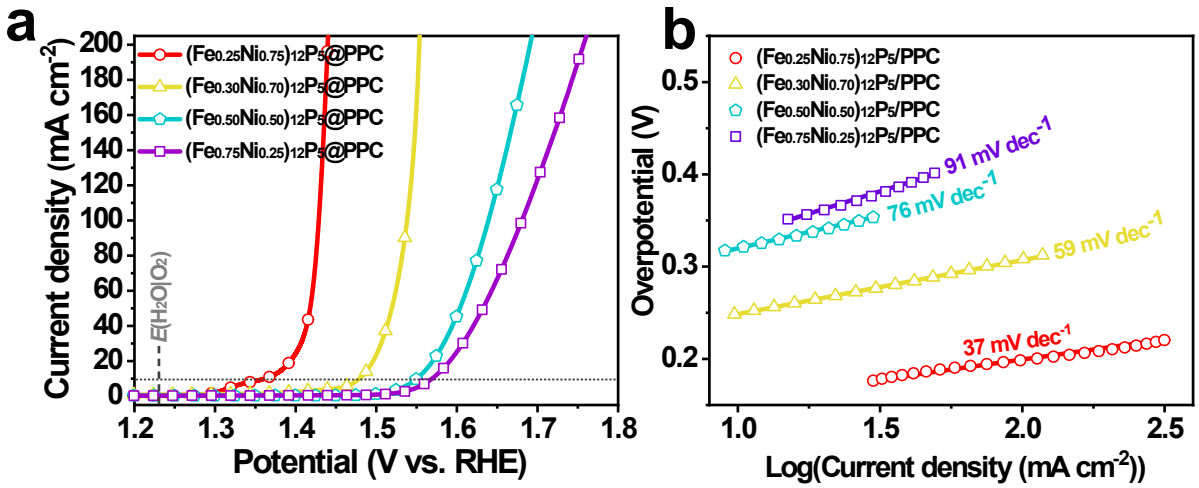

Fig. S8 (a) OER polarization curves of the samples with Fe amount over 0.25 in $(Fe_xNi_y)_{12}P_5$@PPC measured in 1.0 M KOH solution (pH=14) with a scan rate of 5.0 mV s^{-1} with 95% iR-correction. (b) Tafel plotsderived from corresponding OER polarization curves.

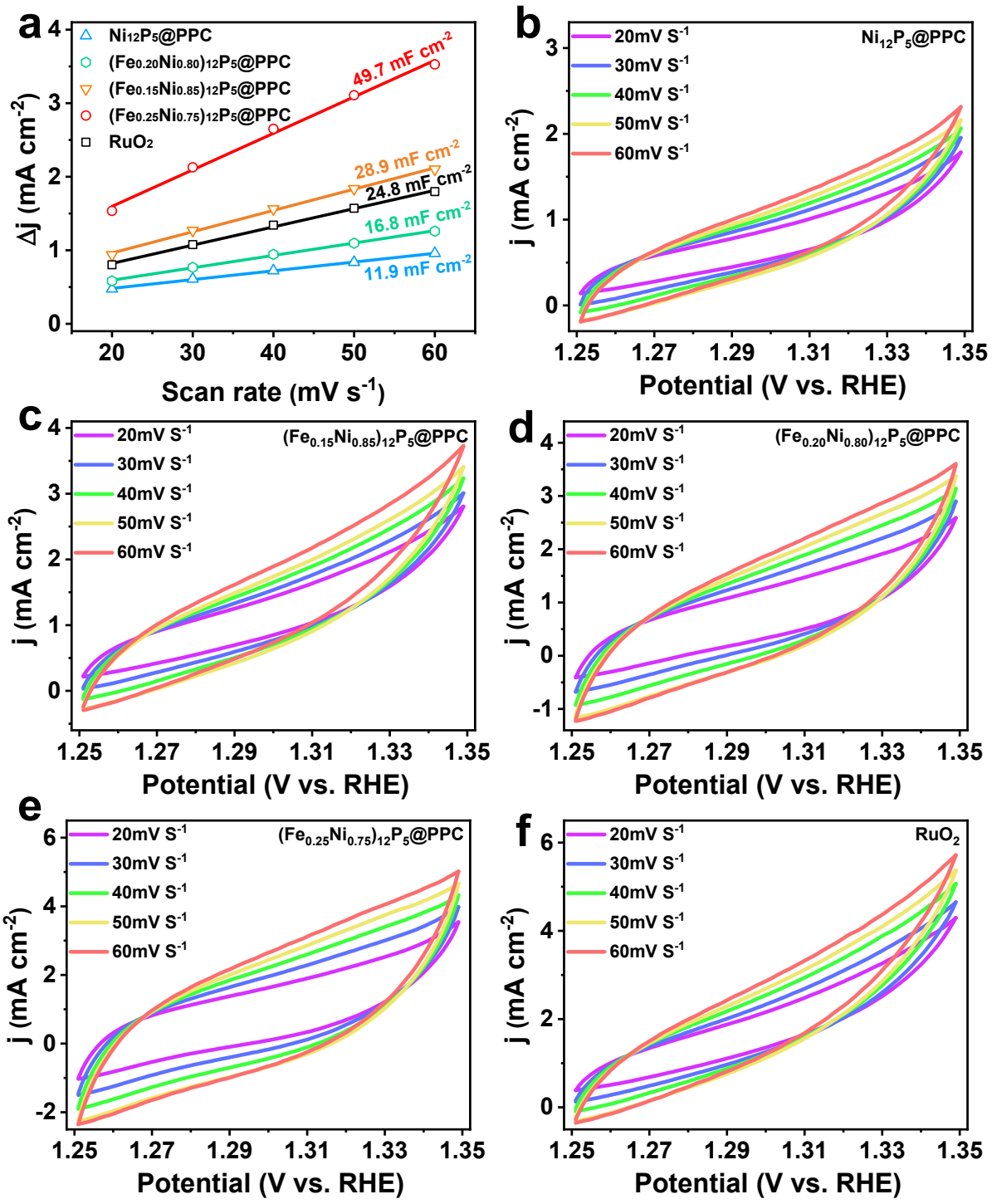

Fig. S9 (a) Scan rate dependence of current density for the catalysts at 1.30 V *vs.* RHE. CV curves at different scan rates for (b) $Ni_{12}P_5$@PPC, (c) $(Fe_{0.15}Ni_{0.85})_{12}P_5$@PPC, (d) $(Fe_{0.20}Ni_{0.80})_{12}P_5$@PPC, (e) $(Fe_{0.25}Ni_{0.75})_{12}P_5$@PPC, and (f) RuO_2.

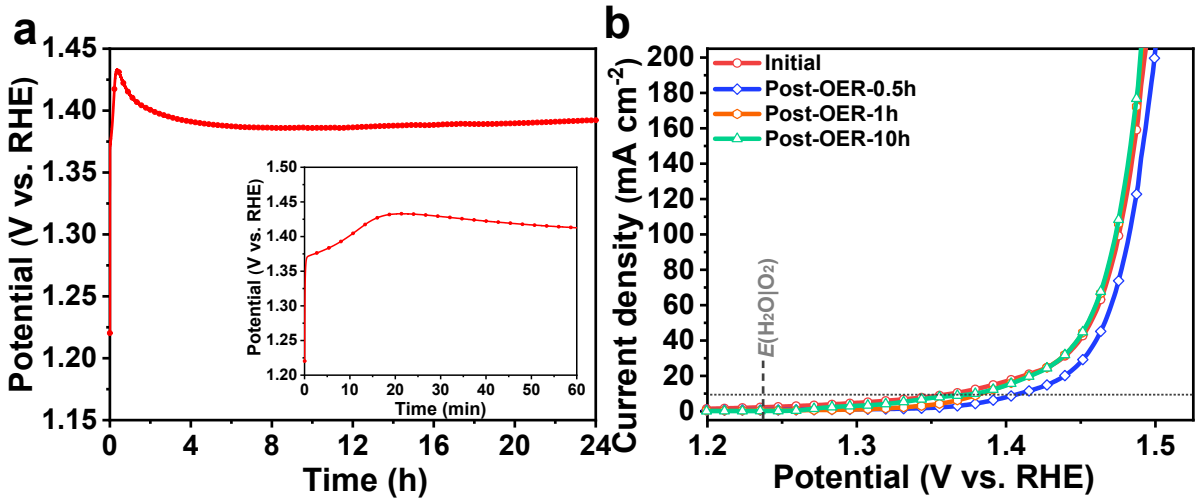

Fig. S10 (a) Chronopotentiometry curve of $(Ni_{0.75}Fe_{0.25})_{12}P_5$@PPC at a constant current density of 10 mA cm^{-2} for a total duration of 24 h (inset of corresponding partial enlarged view), (b) LSV curves (with a scan rate of 5.0 mV s^{-1} and 95% iR-correction) before and after 0.5 h, 1 h and 10 h OER tests.)

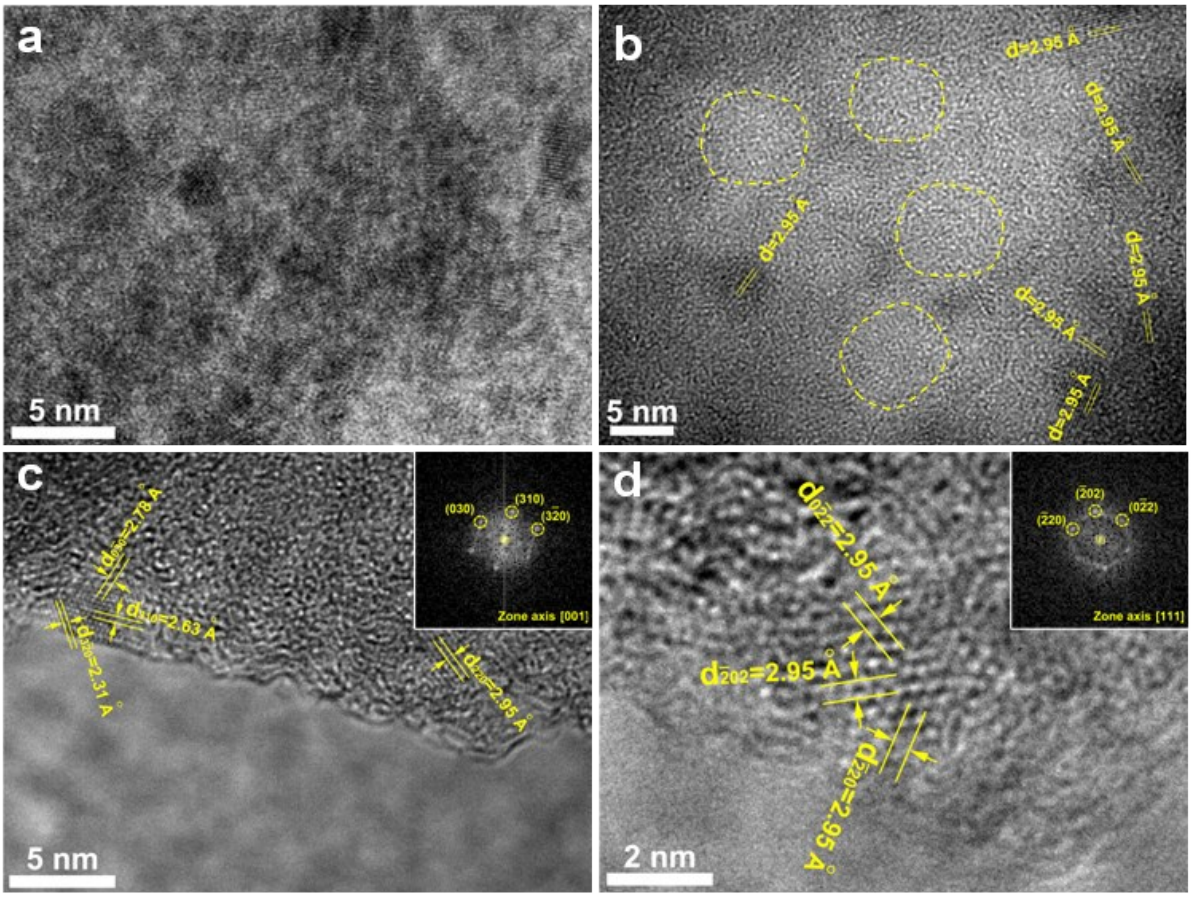

Fig. S11 (a), (b), (c) and (d) HRTEM images of Post-OER-10h sample. (insets of c, d: corresponding FFT patterns along [001] and[111] zone axes).

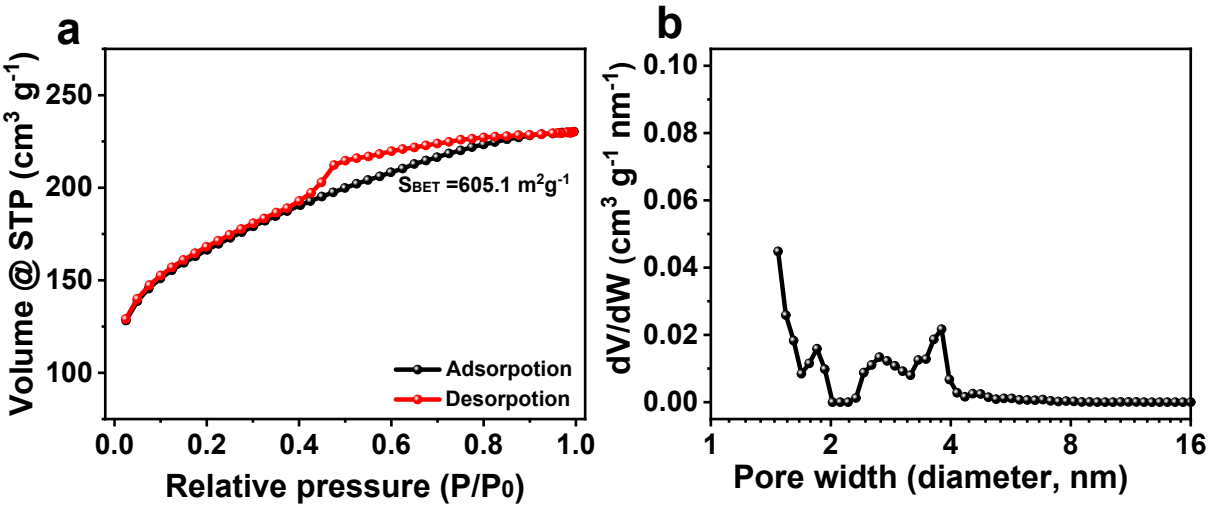

Fig. S12 (a) N_2 adsorption-desorption isotherm and (b) Corresponding DFT pore size distribution curve of Post-OER-10h sample.

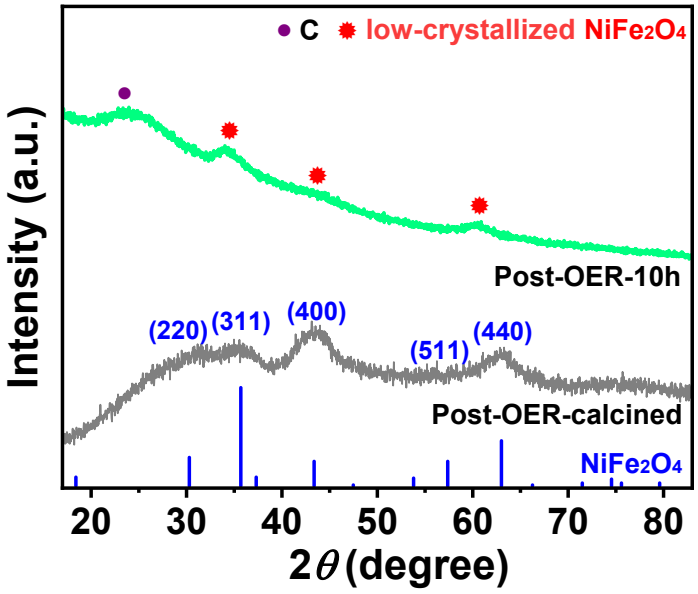

Fig. S13 XRD patterns of Post-OER-10h sample and corresponding calcined (Post-OER-calcined) sample (annealed at 350 ℃ under N_2 atmosphere for 1 h).

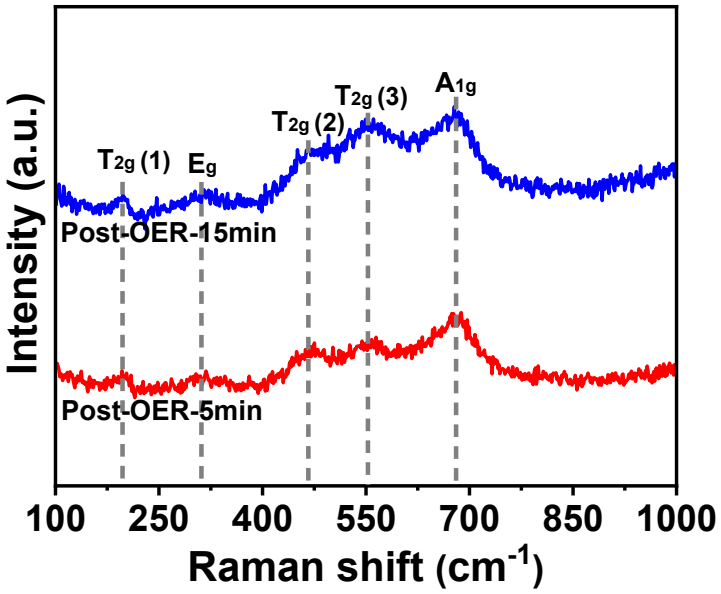

Fig. S14 Raman spectra of Post-OER-5min and Post-OER-15min samples.

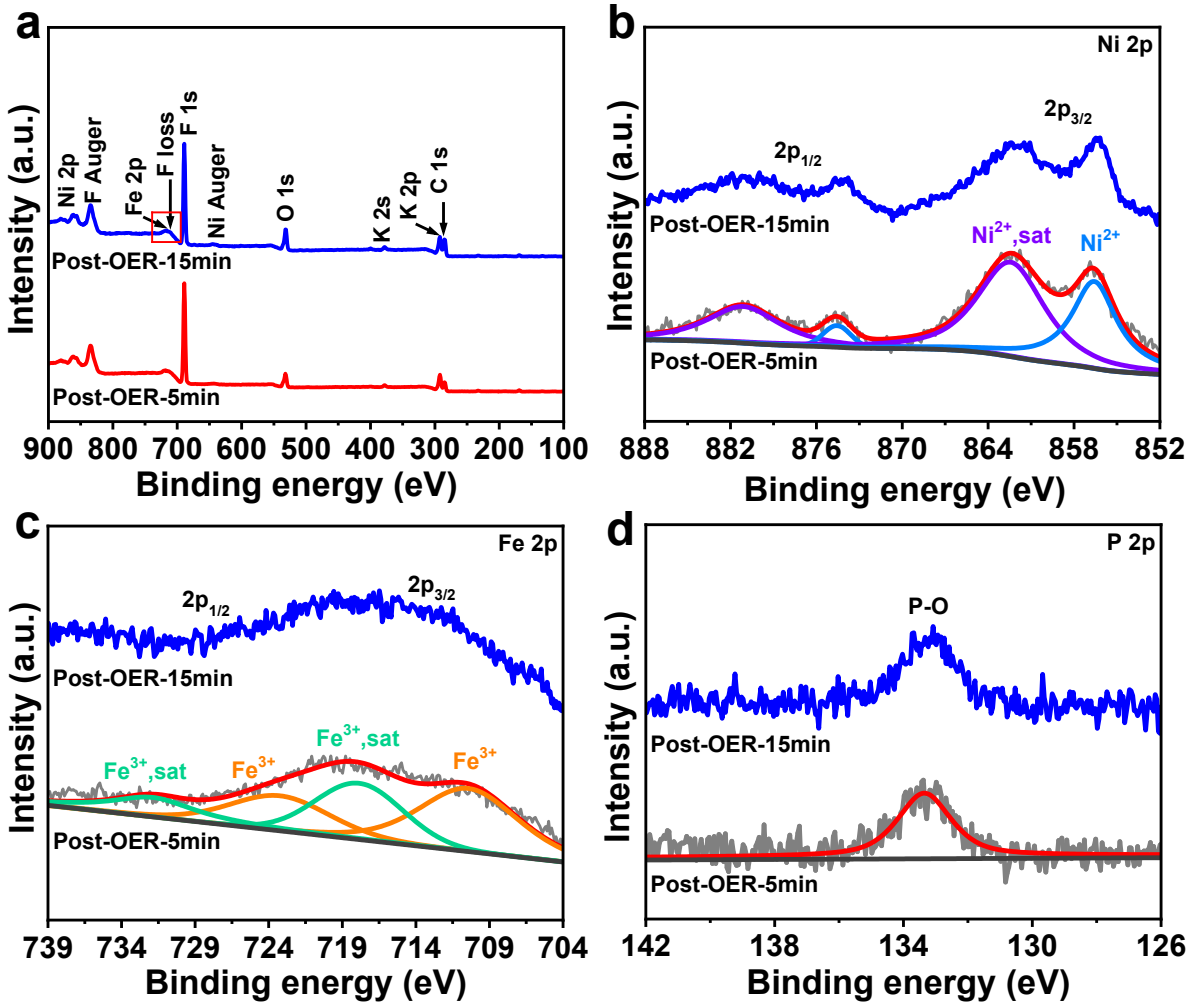

Fig. S15 (a) XPS survey spectrum and (b) Corresponding high-resolutionNi 2p, (c) Fe 2p, and (d) P 2p XPS spectra of Post-OER-5min and Post-OER-15min samples.

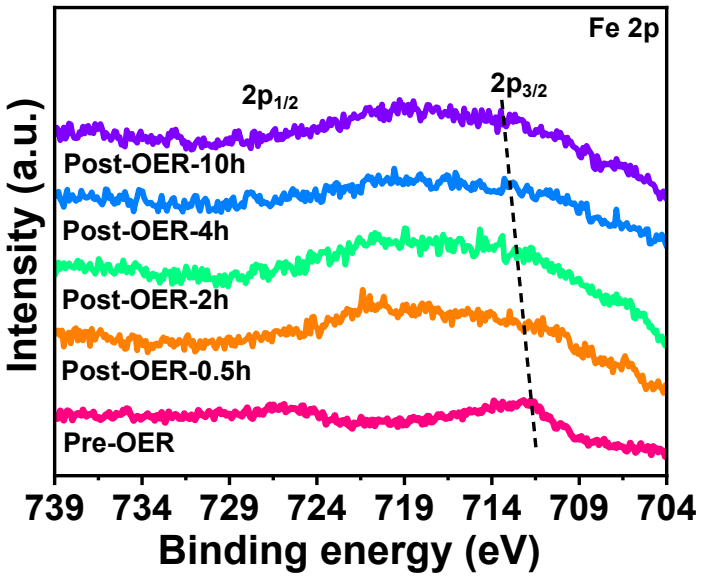

Fig. S16 Fe 2p XPS spectra of Pre-OER and Post-OER-*t* samples.

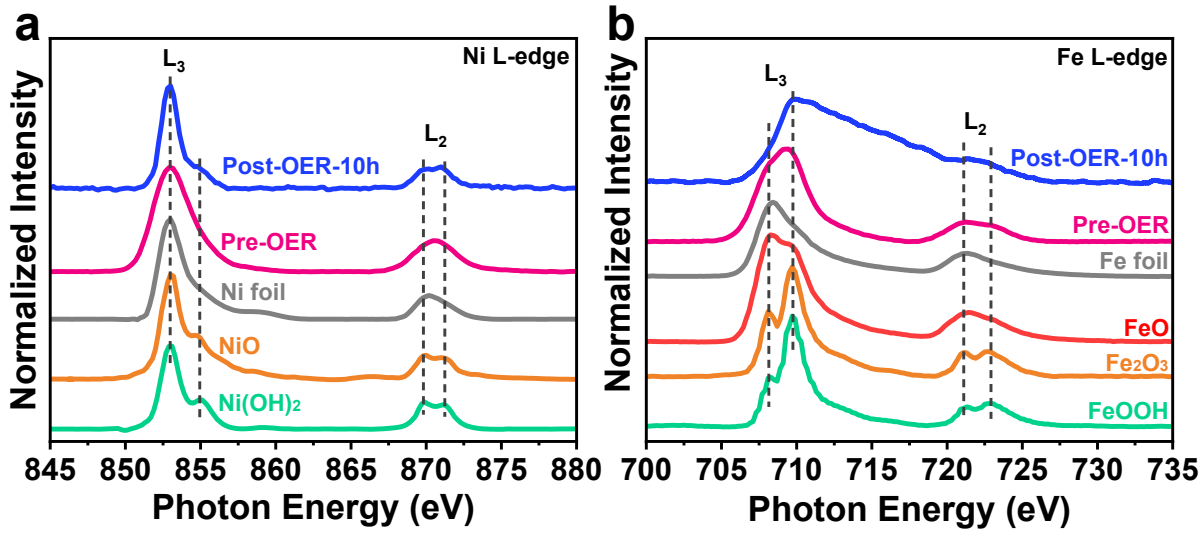

Fig. S17 (a) Ni L-edge and (b) Fe L-edge NEXAFS of Pre-OER and Post-OER-10h samples.

Table S1. Comparison of the OER performances (measured in 1.0 M KOH) for different electrocatalysts.

Catalysts	η_{10}(mV)	Tafel slope(mV/dec)	Reference
NiFe-LDH/CNT	220	31	*J Am Chem Soc, **2013**, 135, 8452.*
CF@NiP_x	200	54.7	*J. Mater. Chem. A, **2016**, 4, 9691.*
NiFeS/NF	189	65	*J. Mater. Chem. A, **2016**, 4, 13499.*
Ni_3FeN-NPs	280	46	*Advanced Energy Materials, **2016**, 6, 1502585.*
Fe-Ni-P/RGO	240	63	*ACS Applied Materials & Interfaces, **2017**, 9, 23852.*
$Ni_2P(O)/Fe_2P(O)$	179	42.7	*ACS Energy Letters, **2017**, 2, 2257.*
$(Fe_{0.5}Ni_{0.5})_2P$/NF	156	66	*Nano Energy, **2017**, 38, 553.*
bulk amorphous NiFeP	219	32	*Advanced Materials, **2017**, 29, 1606570.*
$(Ni_{0.5}Fe_{0.5})_2P$	203	57	*J. Mater. Chem. A, **2017**, 5, 11229.*
Co4Ni1P	245	61	*Advanced Functional Materials, **2017**, 27, 1703455.*
a-NiFe-OH/NiFeP/NF	199	39	*ACS Energy Letters, **2017**, 2, 1035.*
CoNi(20:1)-P-NS	209	52	*Energy & Environmental Science, **2017**, 10, 893.*
Fe−Co−P	252	33	*ACS Nano, **2018**, 12, 158.*
Ni_2Fe_1-O	244	39	*Advanced Energy Materials,**2018**, 8,1701347.*
IrO_2@Ir	255	45	*Nanoscale, **2019**, 11, 4407.*
H-NiFe-LDH	184	62.3	*Energy & Environmental Science, **2019**, 12, 572.*
Cr-FeNi-P/NCN	240	72.4	*Advanced Materials, **2019**, 31, 1900178.*
a-LNF(t-d)	189	36	*Advanced Materials, **2019**, 31, 1900883.*
FeP_2-NiP_2@PC	248	54	*ACS Appl Mater Interfaces, **2019**, 12, 727.*
NiFe-NFF	227	38.9	*Advanced Functional Materials, **2019**, 29, 1807418.*
FeNiP/C-900	229	74.5	*Nano Energy, **2019**, 62, 745.*
$FeNi_3$@NC	277	77	*Applied Catalysis B: Environmental, **2020**, 268, 118729.*
FeOOH/Ni_3N	244	65	*Applied Catalysis B: Environmental, **2020**, 269, 118600.*
$(Ni_xFe_{1-x})_2P$	166	59.3	*ACS Catalysis, **2020**, 10, 9086.*
$(Fe_{0.25}Ni_{0.75})_{12}P_5$@PPC	131	37	This work

Table S2. The results of ICP-AES and corresponding amount of metal atoms.

Samples	ICPdetermined Element content(%)			Element content of metal working electrode (μmol)		
	Ni	Fe	Total [a]	Ni	Fe	Total [a]
$(Fe_{0.25}Ni_{0.75})_{12}P_5$@PPC	15.7	4.9	20.6	5.4	1.8	7.2
$(Fe_{0.20}Ni_{0.80})_{12}P_5$@PPC	16.4	3.9	20.3	5.7	1.4	7.1
$(Fe_{0.15}Ni_{0.85})_{12}P_5$@PPC	17.4	3.3	20.7	6.0	1.1	7.1
$Ni_{12}P_5$@PPC	20.5	0	20.5	7.0	0	7.0
IrO_2	-	-	76.0	-	-	15.0

[a] Total metal content in the samples.

Table S3. Comparison of OER activity of different catalysts.

Catalysts	η_{10} (mV)	η_{100} (mV)	Tafel slope (mV/dec)	C_{DL} (mF cm^{-2})	ESCA (cm^2)	j at η = 0.25V (mA cm^{-2})	TOF at η = 0.25V (s^{-1})
$Ni_{12}P_5$@PPC	302	400	96	6.0	145.0	7.1	0.003
$(Fe_{0.15}Ni_{0.75})_{12}P_5$@PPC	269	363	93	8.4	210.0	6.5	0.002
$(Fe_{0.20}Ni_{0.80})_{12}P_5$@PPC	237	330	83	14.5	362.5	14.6	0.005
$(Fe_{0.25}Ni_{0.75})_{12}P_5$@PPC	131	198	37	24.9	622.5	422.0	0.156
RuO_2	227	322	113	12.4	310.0	19.4	0.003

The ECSA values of the catalysts were calculated according to the following equation:

$$ECSA = C_{dl}/C_s$$

where C_{dl} is double layer capacitance determined by CV curves at the non-Faradaic region (1.25-1.35 V *vs.* RHE) with diffrent scan rates (20 to 60 mV s^{-1}), and C_s is the specific capacitance value of an ideal flat surface with a real surface area of 1.0 cm^2. In this work, C_{dl} was estimated as half of the linear slope of charging current density differences (ΔJ) against the scan rates plots (Fig. S9a), and C_s was taken the general value of 0.04 mF (the calculation refers to *J. Am. Chem. Soc.* ***2013****, 135, 16977*) .

The turnover frequency (TOF) was calculated according to the following equation:

$$TOF = (j \times A)/(4 \times n \times F)$$

where j is the current density obtained at 1.48 V (*vs.* RHE), A is the surface area of the working electrode (1.0 cm^2), F is the Faraday efficiency (96485 C mol^{-1}) and n is the number of moles of metal (by assuming every metal atom to be catalytically active) loaded on the working electrodes (listed in Table S2) (the calculation refers to *Chem. Sci.,* ***2011****, 2, 1262*).

Table S4. Spectroscopy parameters of samples at room temperature.

Samples	Component	Isomer shift (δ, mm s^{-1})	Quadrupole splitting (Δ, mm s^{-1})	H_{hf} (T)	Assignment	Area (%)
Pre-OER	Para, Fe^{2+}	1.37	2.74	-	-	14.3
	Para, Fe^{3+}	0.35	0.88	-	-	85.7
Post-OER-0.5h	Para, Fe^{3+}	0.42	0.58	-	-	50.1
	Para, Fe^{4+}	-0.09	-	-	-	4.9
	Mag, Fe^{3+}	0.31	0.04	48.5	$NiFe_2O_4$	22.5
	Mag, Fe^{3+}	0.72	0.17	52.1		22.5
Post-OER-2h	Para, Fe^{3+}	0.38	0.65	-	-	71.8
	Para, Fe^{4+}	-0.10	-	-	-	11.3
	Mag, Fe^{3+}	0.28	0.04	48.9	$NiFe_2O_4$	16.9
Post-OER-4h	Para, Fe^{3+}	0.35	0.51	-	-	86.2
	Para, Fe^{4+}	-0.10	-	-	-	13.8
Post-OER-10h	Para, Fe^{3+}	0.38	0.62	-	-	85.8
	Para, Fe^{4+}	-0.10	-	-	-	14.2